

# Flow at the SPS and RHIC as a Quark-Gluon Plasma Signature

D. Teaney<sup>1</sup>, J. Lauret<sup>2</sup>, E.V. Shuryak<sup>1</sup>

<sup>1</sup> *Department of Physics and Astronomy,* <sup>2</sup> *Department of Chemistry,*  
*State University of New York at Stony Brook, NY 11794-3800,*

(February 8, 2008)

Radial and elliptic flow in non-central heavy ion collisions can constrain the effective Equation of State(EoS) of the excited nuclear matter. To this end, a model combining relativistic hydrodynamics and a hadronic transport code(RQMD [1]) is developed. For an EoS with a first order phase transition, the model reproduces both the radial and elliptic flow data at the SPS. With the EoS fixed from SPS data, we quantify predictions at RHIC where the Quark Gluon Plasma(QGP) pressure is expected to drive additional radial and elliptic flow. Currently, the strong elliptic flow observed in the first RHIC measurements does not conclusively signal this nascent QGP pressure. Additional measurements are suggested to pin down the EoS.

1. By colliding heavy nuclei at the SPS and RHIC accelerating facilities, physicists hope to excite hadronic matter into a new phase consisting of deconfined quarks and gluons – the Quark Gluon Plasma(QGP) [2]. After the collision, the produced particles move collectively or *flow* and this flow may quantify the effective Equation of State(EoS) of the matter. In central PbPb collisions at the SPS, a strong radial flow is observed [3]. The matter develops a collective transverse velocity approaching  $(1/2)c$ . In non-central collisions, a radial and an *elliptic* flow are observed [4–6]. Since in non-central collisions the initial nucleus-nucleus overlap region has an elliptic shape, the initial pressure gradient is larger along the impact parameter and the matter moves preferentially in this direction [7].

The phase transition to the QGP influences both the radial and elliptic flows. QCD lattice simulations show an approximately 1st order phase transition [8]. Over a wide range of energy densities  $e = .5 - 1.4 \text{ GeV}/\text{fm}^3$ , the temperature and pressure are nearly constant. Over this range then, the ratio of pressure to energy density  $p/e$ , decreases and reaches a minimum at a particular energy density known as the *softest point*,  $e_{sp} \approx 1.4 \text{ GeV}/\text{fm}^3$  [9]. When the initial energy density is close to  $e_{sp}$ , the small pressure (relative to  $e$ ) cannot effectively accelerate the matter. However, when the initial energy density is well above  $e_{sp}$ ,  $p/e$  approaches  $1/3$ , and the larger pressure drives collective motion [9,10]. At a time of  $\sim 1 \text{ fm}/c$ , the energy densities at the SPS( $\sqrt{s}_{NN} = 17 \text{ GeV}$ ) and RHIC ( $\sqrt{s}_{NN} = 130 \text{ GeV}$ ) are very approximately 4 and  $7 \text{ GeV}/\text{fm}^3$  respectively [11,12]. Based on these experimental estimates, the hard QGP phase is expected to live significantly longer at RHIC than at the SPS. The final flows of the produced particles should reflect this difference. In this paper we pose the question: Can both the radial and elliptic flow at the SPS and RHIC be described by a single effective EoS?

Since the various hadron species have different elastic cross sections, they freezeout (or decouple) from the hot fireball at different times [13]. Because flow builds up over time, it is essential to model this differential freezeout. It was ignored in previous hydrodynamic simulations of non-central heavy ion collisions and elliptic flow

was over-predicted flow by a factor of two [14,15].

2. The Hydro to Hadrons(H2H) model will be described in detail elsewhere [16]. Other authors have previously constructed a similar model for central collisions [17]. The model evolves the QGP and mixed phases as a relativistic fluid, but switches to a hadronic cascade (RQMDv2.4 [1]) at the beginning of the hadronic phase to model differential freezeout. The computer code consists of three distinct components. Assuming Bjorken scaling, the first component solves the equations of relativistic hydrodynamics in the transverse plane [7] and constructs a switching surface at a temperature,  $T_{switch} = 160 \text{ MeV}$ . The second component generates hadron on the switching surface using the Cooper-Frye formula [18] with a theta function rejecting backward going particles [19,20]. Finally, the third component (RQMD) sequentially re-scatters the generated hadrons until freezeout.

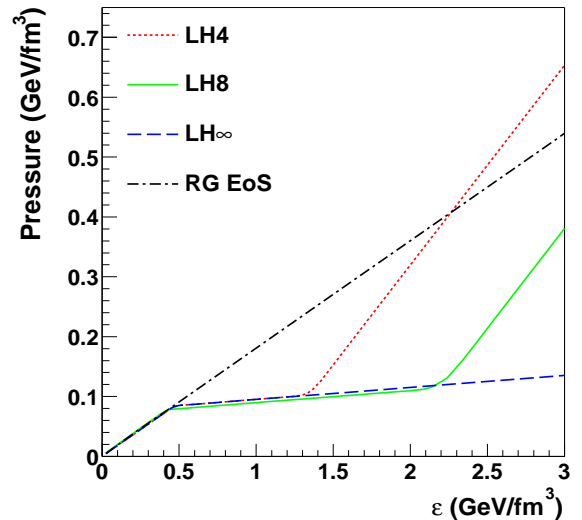


FIG. 1. The pressure versus the energy density( $\epsilon$ ) for different EoSs (see text). EoSs with Latent Heats  $0.4 \text{ GeV}/\text{fm}^3$ ,  $0.8 \text{ GeV}/\text{fm}^3$ ,... are labeled as LH4, LH8,...etc.

For the hydrodynamic evolution, a family of EoSs was constructed with an adjustable Latent Heat(LH)

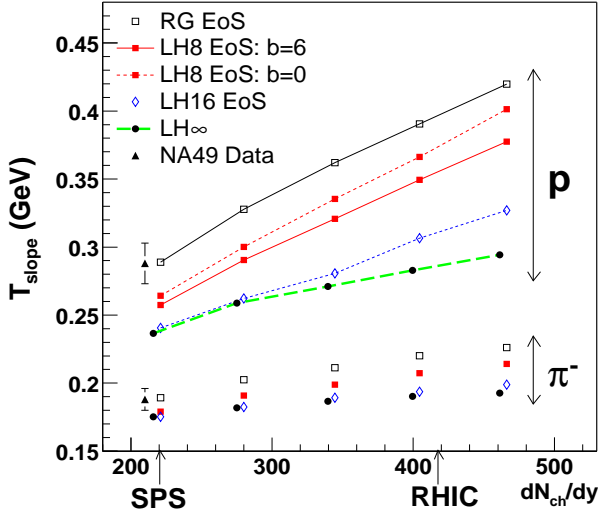


FIG. 2. The transverse mass slope ( $T_{slope}$ ) as a function of the total charged particle multiplicity in PbPb collisions at an impact parameter of  $b=6$  fm (see also [10,17]). For consistency with the elliptic study in Fig. 3, we show  $b=6$  fm although the NA49 data points [21] are for the 5% most central events, or  $b < 3.5$  fm. For all EoSs at the SPS, the proton slope parameters at  $b=6$  fm are  $\approx 7$  MeV smaller than at  $b=0$  fm, as for the  $b=0$  LH8 curve. The difference is negligible for  $\pi^-$ .

(see Fig. 1).  $LH_\infty$  is considered as a limiting case, mimicking non-equilibrium phenomena [22]. The hadron phase exists up to a critical temperature of  $T_c = 165$  MeV, and consists of ideal gas mixture of the meson pseudoscalar and vector nonets and the baryon octet and decuplet. The hadron phase is followed by a mixed phase with a specified LH, which is finally followed by a QGP phase with  $C_s^2 = 1/3$ . In addition, a Resonance Gas (RG) EoS was constructed with a constant speed of sound above the hadron phase.

3. *Radial flow* is quantified experimentally by slope parameters,  $T_{slope}$ ; the momentum spectrum of each particle is fit to the form  $dN/dM_T^2 dy|_{y=0} = C e^{-M_T/T_{slope}}$  where  $M_T^2 = P_T^2 + m^2$ .  $T_{slope}$  incorporates random thermal motion and the collective transverse velocity.

In Fig. 2, the pion and proton slope parameters are plotted as functions of the total charged particle multiplicity in the collision. Look first at the leftmost points at SPS multiplicities and compare the model and experimental slopes: The proton slope data favor a relatively hard EoS – LH8 or harder. A direct comparison of the model to published spectra [23] supports this claim [16]. A RG EoS can also reproduce the proton flow. A similar analysis of elliptic flow (shown and quantified below) favors a relatively soft EoS – LH8 or softer. With some caveats, LH8 represents a happy middle which can reproduce both the radial and elliptic flow at the SPS.

Look now at the energy/multiplicity dependence of the slopes. For all EoSs,  $T_{slope}$  increases with the collision energy [10,17]. For a soft EoS (e.g.  $LH_\infty$ ) the increase is

small and for a hard EoS (e.g. LH8) the increase is large. At RHIC multiplicities, the difference between the slope parameters is large and easily experimentally observable.

4. *Elliptic flow* is quantified experimentally by the elliptic flow parameter,  $v_2 = \langle \cos(2\Phi) \rangle$ ; here  $\Phi$  is the angle around the beam measured relative to the impact parameter and  $\langle \rangle$  denotes an average over the single particle distribution,  $\frac{dN}{dP_T d\Phi}$ .  $v_2(P_T)$  is found by holding  $P_T$  constant in while averaging  $\cos(2\Phi)$  over  $\frac{dN}{dP_T d\Phi}$ .  $v_2$  measures the response of the fireball to the the spatial deformation of the overlap region, which is usually quantified in a Glauber model [24] by the eccentricity  $\epsilon = \langle \langle y^2 - x^2 \rangle \rangle / \langle \langle x^2 + y^2 \rangle \rangle$ . Since the response ( $v_2$ ) is proportional to the driving force ( $\epsilon$ ), the ratio  $v_2/\epsilon$  is used to compare different impact parameters and nuclei [25,26].

In Fig. 3(a), the number elliptic flow ( $v_2$ ) is plotted as a function of charged particle multiplicity at an impact parameter of 6 fm. Before studying the energy dependence, look at the magnitude of the elliptic flow at the SPS. For LH8, the stars show the pion  $v_2$  when the matter is evolved as a fluid until a decoupling temperature of  $T_f = 120$  MeV; they illustrate the excessive elliptic flow typical of pure hydrodynamics. Once a cascade is included, LH8 (the squares) is only  $\approx 20\%$  above the data – a substantial improvement. Typically in hydrodynamic calculations, the freezeout temperature  $T_f$  is adjusted to fit the proton  $P_T$  spectrum. However, protons are driven by a pion “wind” and decouple from the fireball  $5$  fm/c after the pions on average. This pion wind accounts for the strong proton flow at the SPS and is not described by ideal hydrodynamics [17,16]. In order to match the observed proton flow, hydrodynamic calculations must decouple at low freezeout temperatures,  $T_{frz} \approx 120$  MeV/c. This low temperature has two consequences for elliptic flow: First the reduction of elliptic flow due to resonance decays is small  $\approx 15\%$ , compared to  $\approx 30\%$  in the H2H model. Second, compared to a cascade, the hydrodynamics generates twice as much elliptic flow during the late cool hadronic stages of the evolution. By including the pion “wind”, and more generally by decoupling differentially, we can simultaneously describe the radial and elliptic flow data at the SPS.

The energy dependence of  $v_2$  is the central issue. As seen in Fig. 3, the H2H model predicts an increase in elliptic flow by a factor  $\approx 1.4$  and is in reasonable agreement with SPS and RHIC flow data. This result was presented prior to the publication of RHIC data [20]. In contrast, UrQMD, a hadronic cascade based on string dynamics, predicts a decrease by a factor of  $\approx 2$  [27]. This is because the UrQMD string model has a super-soft EoS at high energies [28]. For pure hydrodynamics as illustrated by the stars,  $v_2$  is approximately constant [14] (but see [15]). For HIJING [29], a model which considers only the initial parton collisions,  $v_2$  is  $\approx 0$  [30]. The first RHIC data clearly contradict these models.

The increase in  $v_2$  is now used to constrain the EoS of the excited matter. The QCD phase diagram has two

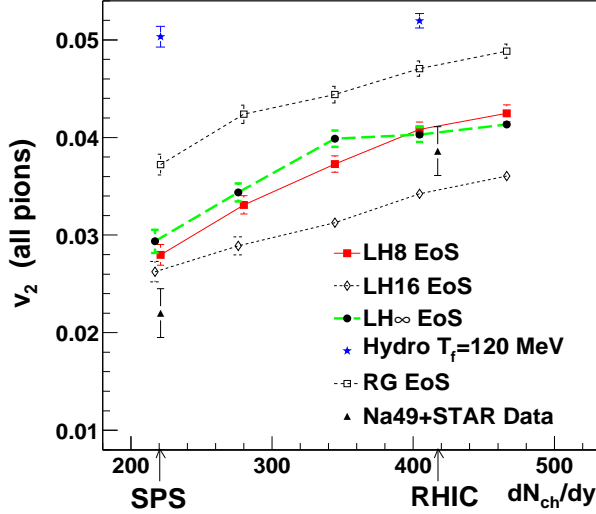


FIG. 3. (a) The number elliptic flow parameter  $v_2$  as a function of the charged particle multiplicity in PbPb collisions at an impact parameter of  $b=6$  fm. At the SPS, the NA49  $v_2$  data point is extrapolated to  $b=6$  fm using Fig. 3 in [5]. At RHIC, the STAR  $v_2$  data point is extrapolated to  $N_{ch}/N_{ch}^{max} = 0.545$  ( $b=6$  fm in AuAu) using Fig. 3 in [6]. The comparison to data is a little unfair: For the model,  $v_2$  is calculated using all pions in PbPb collisions. For the NA49 data,  $v_2$  is measured using only  $\pi^-$  in PbPb (a -3% correction to the model). For the STAR data,  $v_2$  is measured using charged hadrons in AuAu (a +5% correction to the model).

distinguishing features. It is soft at low energy densities and subsequently hard at high energies. A RG EoS (the open squares) has no softness and the elliptic flow is clearly too strong both at the SPS and RHIC. The entire family of EoSs, LH8 through LH $\infty$ , reproduces the elliptic flow data in both energy regimes. Counter-intuitively, as the latent heat is increased,  $v_2$  first decreases and then increases. In the final count, LH8 and LH $\infty$  have roughly the same  $v_2$ . However, they develop the  $v_2$  in different ways. For LH8, the EoS shifts from hard to soft and the early pressure starts an early elliptic expansion. For LH $\infty$ , the EoS is just soft and the elliptic expansion stalls. However because the expansion is stalled, the LH $\infty$  collision lifetime ( $\approx 13$  fm/c at RHIC) is significantly longer than the LH8 lifetime ( $\approx 9$  fm/c at RHIC) [9]. Over the long LH $\infty$  lifetime,  $v_2^{LH\infty}$  steadily grows and is finally comparable to  $v_2^{LH8}$ . As the latent heat is increased from LH8 to LH16, the EoS becomes softer and  $v_2$  at first decreases. However, as the EoS is made softer still, the lifetime increases and  $v_2$  rises again.

**5. Impact Parameter Dependence.** In Fig. 4,  $v_2$  for LH8 as a function of the number participants ( $N_p$ ) is compared to data. Different EoSs show a similar participant (or b) dependence. The agreement is good at RHIC where the multiplicity is high. For ideal hydrodynamics,  $v_2 \propto \epsilon \propto (N_p^{max} - N_p)$  [7]. In the low density limit, since the

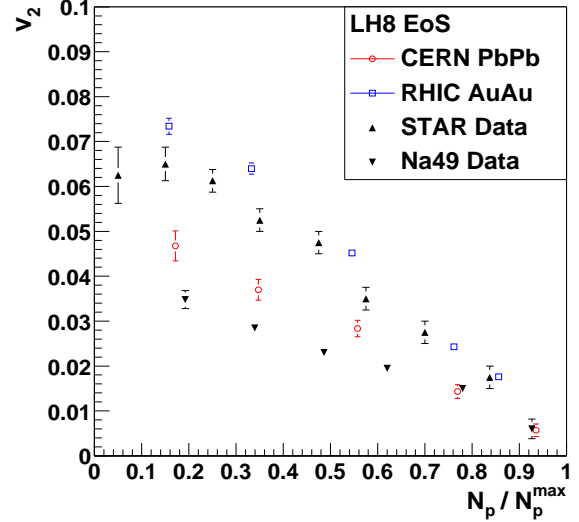


FIG. 4.  $v_2$  versus the number of participants ( $N_p$ ) relative to the maximum. The model and the NA49  $v_2$  values [5] at the SPS are for  $\pi^-$ . The NA49 data are mapped from  $b$  to participants using [31]. The model and the STAR  $v_2$  values [6] at RHIC are for charged particles. The model does not include weak decays. The number of charged particles is assumed proportional to  $N_p$ .

response is proportional to the number of collisions,  $v_2 \propto \epsilon \frac{dN}{dy} \propto (N_p^{max} - N_p)N_p$ . Therefore,  $v_2$  has a different  $N_p$  (or  $b$ ) dependence in the hydrodynamic and low density limits [25,26]. At RHIC, except in very peripheral collisions, the  $N_p$  dependence is clearly linear and strongly supports the hydrodynamic limit [6]. At the SPS, the  $N_p$  dependence may not be clearly linear, but it also does not follow the low density limit. Two-pion correlations, may change the data analysis [32], reduce  $v_2$  in the periphery and improve the low density agreement.

Finally in Fig. 5,  $v_2$  is studied both as a function of transverse momentum and impact parameter. For both LH8 and LH $\infty$ , the calculation produces too much elliptic flow in peripheral collisions (45-85%), and too little elliptic flow in the most central collisions (0-11%). The  $P_T$  dependence of  $v_2$  also clarifies the difference between LH8 and LH $\infty$ : LH $\infty$ , a super soft EoS, generates elliptic flow only at low momentum while LH8, a hard EoS, generates elliptic at high momentum.

**6. Summary and Discussion.** By incorporating differential freezeout, the Hydro to Hadrons (H2H) model simultaneously reproduces the radial and elliptic flow at the SPS and RHIC. At the SPS, the radial flow demands an EoS with a latent heat  $LH \gtrsim 0.8$  GeV/fm $^3$ , while elliptic flow demands an EoS with a latent heat  $LH \lesssim 0.8$  GeV/fm $^3$ . Further, in contrast to string and collision-less parton models, the increase in  $v_2$  is naturally explained using hydrodynamics. This challenges the prevailing view [6,26] that the SPS is in the low density regime and that the increase in  $v_2$  represents a transition

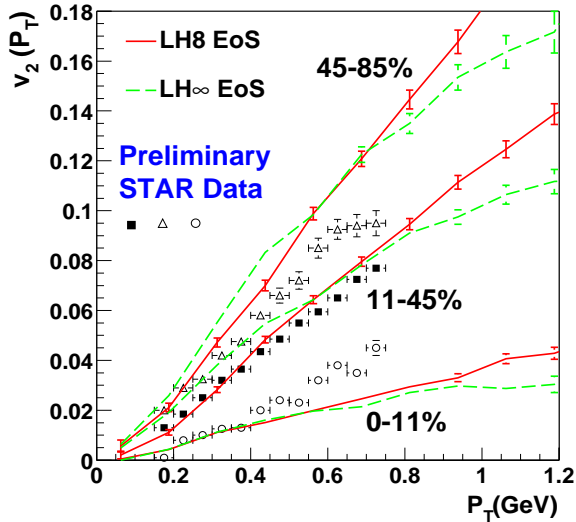


FIG. 5. Elliptic flow of charged pions as a function of  $P_T$  and centrality for AuAu collisions at RHIC. For centrality selections The percentages shown 0-11%, 11-45% and 45-85%, indicate the fraction of the total geometric cross section for three centrality selections  $0\text{ fm} < b < 4.2\text{ fm}$ ,  $4.2\text{ fm} < b < 8.4\text{ fm}$  and  $8.4\text{ fm} < b < 11.6\text{ fm}$ . The preliminary data points were presented in [33,34]. The model curves were found by parameterizing the model data points and averaging over the specified impact range with the geometric weight,  $2\pi b db$ .

to the hydrodynamic regime. However, the increase in  $v_2$  does not uniquely signal the asymptotic QGP pressure. Indeed, at RHIC collision energies, a very soft EoS can have the same  $v_2$  as an EoS with a well developed QGP phase. This EoS is not academic since softness can mimic non-equilibrium phenomena [22]. To reveal the underlying EoS and the burgeoning QGP pressure, the collision energy should be scanned from the SPS to RHIC. If the prevailing low density view of the SPS is correct, a transition in the  $b$  dependence of elliptic flow should be observed over the energy range [25,26]. In addition, for different EoSs,  $v_2$  depends differently on collision energy and transverse momentum (Fig. 3 and Fig. 5). Taken with the radial flow (Fig. 2), this experimental information would help settle the EoS of hot hadronic matter.

**Acknowledgments.** The work is partly supported by the US DOE grant No. DE-FG02-88ER40388 and grant No. DE-FGO2-87ER 40331.

**Note Added.** After the submission of this work, the STAR and PHENIX collaborations reported proton at anti-proton spectra [33]. The preliminary spectra favor LH8-LH16 and disfavor LH $\infty$  [35].

[1] H. Sorge, Phys. Rev. C **52**, 3291 (1995).  
[2] e.g., E.V. Shuryak, Phys. Rept. **61**, 71 (1980); L. McLerran, Rev. Mod. Phys. **58**, 1021 (1986).

[3] e.g., R. Stock, in QM '99, Nucl. Phys. **A661**, 419c (1999).  
[4] e.g., E895 Collaboration, C. Pinkenburg *et al.* Phys. Rev. Lett. **83**, 1295 (1999); NA49 Collaboration, H. Appelshäuser *et al.*, Phys. Rev. Lett. **80**, 4136 (1998).  
[5] A.M. Poskanzer and S.A. Voloshin for the NA49 Collaboration, Nucl. Phys. **A661**, 341c (1999).  
[6] STAR Collaboration, K.H. Ackermann *et al.*; nucl-ex/0009011.  
[7] J.-Y. Ollitrault, Phys. Rev. **D46**, 229 (1992)  
[8] e.g., M. Oevers, F. Karsch, E. Laermann, and P. Schmidt, Nucl. Phys. Proc. Suppl. **73**, 465 (1999).  
[9] C.M. Hung, E.V. Shuryak, Phys. Rev. Lett. **75**, 4003 (1995); D. H. Rischke and M. Gyulassy, Nucl. Phys. **A608**, 479 (1996).  
[10] M. Kataja *et al.*, Phys. Rev. **D34**, 794 and 2755 (1986).  
[11] NA49 Collaboration, T. Alber *et al.*, Phys. Rev. Lett. **75**, 3814 (1995).  
[12] PHOBOS Collaboration, B.B. Back *et al.*, Phys. Rev. Lett. **85**, 3100 (2000); hep-ex/0007036  
[13] H. Sorge, Phys. Rev. Lett. **81**, 5764 (1998).  
[14] P. Kolb, J. Sollfrank, U. Heinz, Phys. Lett. **B459**, 667 (1999).  
[15] P. Kolb, J. Sollfrank, U. Heinz, preprint hep-ph/0006129.  
[16] D. Teaney, J. Lauret, and E.V. Shuryak, in progress.  
[17] S. Bass and A. Dumitru, Phys. Rev. **C61**, 064909 (2000).  
[18] F. Cooper and G. Frye, Phys. Rev. **D10**, 186 (1974)  
[19] For discussion see, Cs. Anderlik *et al.*, Phys. Rev. **C59**, 388 (1999) and references therein.  
[20] E.V. Shuryak in QM '99, Nucl. Phys. **A661**, 119c (1999); D. Teaney *et al.*, talk at RHIC2000, Park City, Utah, March 10-15 (2000); <http://theo08.nsl.msui.edu/RHIC2k/proceedings.htm>.  
[21] G. Roland for the NA49 Collaboration, Nucl. Phys. **A638**, 91c (1999).  
[22] H. Sorge, Phys. Lett. **B402**, 251 (1997).  
[23] NA49 Collaboration, H. Appelshäuser *et al.*, Phys. Rev. Lett. **82**, 2471 (1999).  
[24] P. Jacobs and G. Cooper, STAR SN402(1999).  
[25] H. Heiselberg and A.-M. Levy, Phys. Rev. **C59**, 2716 (1999).  
[26] S.A. Voloshin and A.M. Poskanzer, Phys. Lett. **B474**, 27 (2000).  
[27] M. Bleicher and H. Stocker, preprint hep-ph/0006147.  
[28] M. Belacem *et al.*, Phys. Rev. **C58**, 1727 (1998).  
[29] M. Gyulassy and X.N. Wang, Comp. Phys. Comm. **83**, 307 (1994); Phys. Rev. **D44**, 3501 (1991).  
[30] R.J.M Snellings, A.M. Poskanzer, S.A. Voloshin, STAR Note SN0388 (1999), preprint nucl-ex/9904003.  
[31] G. Cooper for the NA49 Collaboration, Nucl. Phys. **A661**, 362c (1999).  
[32] P.M. Dinh, N. Borghini, and J.-Y. Ollitrault, Phys. Lett. **B477**, 51 (2000).  
[33] Quark Matter 2001, to be published, Stony Brook, NY, January 15-20 (2001); <http://www.rhic.bnl.gov/qm2001/program.html>  
[34] R. Snellings for the STAR Collaboration, at Quark Matter 2001 [33].  
[35] D. Teaney, at Quark Matter 2001 [33].